Finite-bias visibility dependence in an electronic Mach-Zehnder interferometer

E. Bieri,[1] M. Weiss,[1] O. Göktas,[2] M. Hauser,[2] C. Schönenberger,[1,*] and S. Oberholzer[1]
[1]*Department of Physics, University of Basel, Klingelbergstr. 82, CH-4056 Basel, Switzerland*
[2]*Max-Planck-Institut für Festkörperforschung, Heisenbergstr. 1, D-70569 Stuttgart, Germany*
(Received 31 March 2009; published 23 June 2009)

We use an electronic Mach-Zehnder interferometer to explore the nonequilibrium coherence of the electron waves within the edge states that form in the integral quantum-Hall-effect device. The visibility of the interference as a function of bias voltage and transmission probabilities of the mirrors, which are realized by quantum point contacts, reveals an unexpected asymmetry at finite bias when the transmission probability T of the mirror at the input of the interferometer is varied between 0 and 100%, while the transmission probability of the other mirror at the output is kept fixed. This can lead to the surprising result of an increasing magnitude of interference with increasing bias voltage for certain values of T. A detailed analysis for various transmission probabilities and different directions of the magnetic field demonstrates that this effect is not related to the transmission characteristics of a single-quantum point contact but is an inherent property of the Mach-Zehnder interferometer with edge states.

DOI: 10.1103/PhysRevB.79.245324 PACS number(s): 73.23.−b, 72.70.+m

I. INTRODUCTION

Interferometers, such as the Mach-Zehnder interferometer (MZI),[1,2] play a decisive role in the foundation of physics. They allow to assess and quantify the wave nature of light and matter by probing the complex amplitude of the field.[3] The most simple interferometers are so-called two-path interferometers, of which the MZI (Fig. 1) is a particular symmetric one.[1] Two-path interferometers employ a well-collimated incident beam of light or matter wave generated by source 1, which is then split by a partially transmitting mirror A (beam splitter) with transmission probability T_A and reflection probability $R_A=1-T_A$ into two partial beams. After following two different paths in space, the partial beams are recollected together by a second half mirror B forming two output beams that are measured at detectors 2 and 3. Due to the particle conservation, the two detectors measure complementary intensities. It therefore suffices to consider one detector signal. In case of a fully coherent classical wave with frequency ω, the measured intensity of the output beam is a periodic function of the difference τ in propagation time along the two paths. In the ideal case, the intensity oscillates between zero and a maximum value, in which case one refers to a visibility of 100%.

In recent years, interferometers with a low number of channels have been implemented in nanoelectronic devices lithographically fabricated into high-mobility two-dimensional electron-gas systems.[4] In particular, MZIs (Ref. 5) were realized along these lines.[6–18] The two partial beams are either defined by structuring two paths[6–10] or by using the edge states[11–18] that form in a strong magnetic field in the integer quantum-Hall regime.[19–22] In the former approach, it is difficult to realize a single-quantum channel because of residual backscattering at defects induced, for example, by etching. In contrast, in a strong magnetic field, backscattering is suppressed leading to the formation of chiral edge states. The number of occupied edge states can easily be controlled through the magnetic field. In high-mobility samples of moderate densities, one can even approach a single spin-polarized channel. Edge states as electron beams have the additional advantage that ideal tunable mirrors can be fabricated using quantum point contacts (QPCs).[23,24] In these electronic interferometers, the visibility can be measured by sweeping the phase difference with the aid of the Aharonov-Bohm flux Φ which can be changed either by a

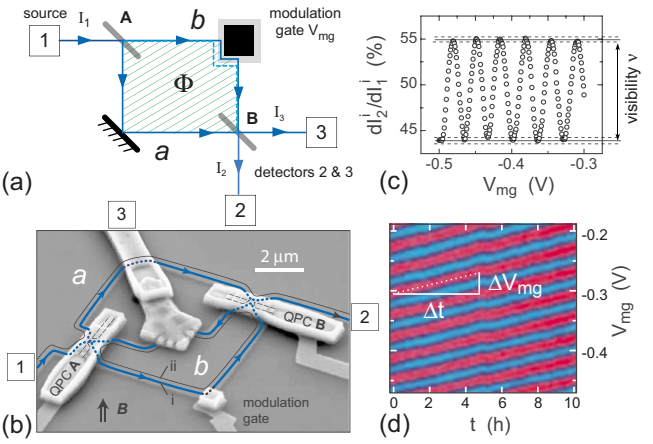

FIG. 1. (Color online) (a) Illustration of a MZI with mirrors A and B, which are characterized by their transmission probabilities T_A and T_B. In the electronic version, a potential V_{mg} at the modulation gate changes the area enclosed by the two partial beams, leading to a phase modulation through the Aharonov-Bohm effect. (b) Experimental implementation of the MZI in a two-dimensional electron gas. The inner Ohmic contact and the two metallic split gates which define QPC A and B are connected via free-standing bridges. Of the two edge states i and ii, only the outer one i is partitioned. The inner edge state ii is fully reflected at the two QPCs. (c) Due to the consequent constructive and destructive interference, the current intensities $I_{2,3}$ at the detector contacts 2 and 3 oscillate as a function of V_{mg}. We measure the differential transmission probability dI_2^i/dI_1^i of the current in the outer edge state i and define the visibility ν as its peak-to-peak modulation as indicated by the solid lines in (c). The dashed lines give an indication for the typical measurement error. (d) Time dependence of the phase of the oscillations.

small variation in the magnetic field or by a variation in the area enclosed by the two paths employing an electrostatic modulation gate V_{mg}.

Previous experiments of the electronic MZI concentrated *either* on the energy dependence of the visibility of a symmetric interferometer ($T_A=T_B=0.5$) *or* on the visibility in linear response for various transmission probabilities. Here, we report on the dependence on $T_{A,B}$ and energy.

In an interaction-free model, the total transmission probability $T_{21} \equiv dI_2/dI_1$ of the MZI consists of two terms:[25] an interference term that depends on the relative phase and a phase-averaged mean transmission probability $\langle T_{21} \rangle$ given by $T_A T_B + R_A R_B$. In the fully coherent case and without dephasing, the amplitude of the interference term is given by

$$\hat{T}_{21} = 2\sqrt{T_A R_A T_B R_B}. \quad (1)$$

We define the visibility ν by the full swing of the interference signal, i.e., $\nu = 2\hat{T}_{21}$ [see Fig. 1(c)]. The visibility is maximal if both mirrors have 50% transparency, i.e., $T_A = T_B = 0.5$. If one transmission probability is varied, ν follows a semicircle dependence.

Two basic symmetries of the visibility are contained in the above equation (1): on one hand, ν is invariant if T_A is exchanged with T_B and, on the other hand, if T_A is changed into $1-T_A$ (or T_B into $1-T_B$). The former more obvious case states that the outcome of the interference experiment does not change if input and output are exchanged. This corresponds to the time-reversal symmetry. The latter says that the visibility is symmetric around a transmission of 50% for both mirrors separately. Whereas the first symmetry is respected in our experiment even at finite bias, we find the second one to be violated. This symmetry breaking, as we will show below, can lead to the remarkable result of an enhancement of the visibility with increasing bias voltage. This is surprising because with increasing energy one would expect that the number of inelastic-scattering channels increases, leading to an enhanced dephasing and therefore reduced visibility. This new feature contrast previous studies of the energy dependence of the visibility which have always reported a decay of the interference amplitude with energy (i.e., applied bias voltage).

II. EXPERIMENTAL

The electronic MZI is implemented in a high-mobility two-dimensional electron gas that forms at the interface of a $GaAs/Ga_{0.7}Al_{0.3}As$ heterojunction 120 nm below the surface with an electron density of $1.6 10^{11}$ cm^{-2} and a mobility of 170 m^2/Vs at 4.2 K without illumination. It is defined by wet-chemical etching of a ring structure combined with two QPCs formed by metallic split gates [Fig. 1(b)]. Due to the chiral nature of the edge states, one of the detector contact lies inside the ring. This current at contact 3 is drained to ground via a small central Ohmic contact. This Ohmic contact as well as the two split gates are connected by freely suspended bridges, which were realized with a two-layer resist technique employing polymethyl methacrylate (PMMA) as the bottom and PMMA-MA as the top layer.

The area A enclosed by the two partial beams, which each have a length of ≈ 15 μm, amounts to $A \approx 38$ μm^2 conducted, the total quanta h/e. All measurements reported here were carried out in a vertical magnetic field of $B = \pm 3.55$ T where two spin-polarized edge states are present (filling factor 2). Of the two edge states, denoted as *i* and *ii* in Fig. 1(b), we only vary the transmission of the *outer* edge state, i.e., of channel *i*, which is the one closest to the sample edge. The inner one is fully reflected at QPC *A* and *B*. A bias modulation technique is applied to deduce the differential transmission probability dI_2/dI_1 or dI_3/dI_1. A small ac modulation V_{ac} of 1 μV is superimposed on the dc voltage V_{dc} and applied to the source contact 1. This contact then injects the current $(e^2/h)V$ into each of the two edge states, where $V = V_{dc} + V_{ac}$. The current at the detector 2 (or 3) is measured over the voltage drop that forms across the detector contact and an additional Ohmic contact connected in series. We then obtain the differential transmission dI_2/dI_1 as the ratio of the respective ac currents. In this relation and in all following ones, we implicitly subtract the current due to the inner edge state. Hence, $I_1 - I_3$ refer in the following to the currents in the outer edge state which we can tune by the QPCs. A result is shown in Fig. 1(c) as a function of the voltage V_{mg} on the modulation gate and in Fig. 1(d) in addition as a function of time. The gradual variation in the phase with time at a rate of $\sim 0.33\pi$/h reflects the decay of the magnetic field of our magnet operated in persistent mode. This results in a change in the magnetic flux Φ that threads the interior of the MZI. Our magnetic field decays with ≈ 18 μT/h, yielding a 2π phase shift every 6 h. Jumps in the phase are absent which indicates a good quality of the heterostructure.

The peak-to-peak amplitude of the interference (the visibility) is extracted from the measured data dI_2/dI_1, such as the one shown in Fig. 1(c), by a statistical method.[16] The data points of the oscillating differential current dI_2/dI_1, which was measured as a function of V_{mg} with equidistant increments, were cast into a histogram. This histogram was then fitted to the form expected from a sinusoidal dependence for dI_2/dI_1 on V_{mg}.[16] As a control, fast Fourier transformation was employed as well. The visibility ν of the coherent oscillations is in our experiments always smaller than 100% with a maximal visibility of 20% at the lowest temperature of 35 mK. As a function of temperature θ, the visibility decays without an indication for saturation at the lowest temperature [see Fig. 3(b)]. The low-temperature decay can be described by an exponential factor $\exp(-k_B \theta \pi / E_c)$,[25] where the characteristic energy term E_c amounts to 2.6 μeV, corresponding to 30 mK. This value agrees within 1 order of magnitude with other reports for similar MZ interferometers. For example, Ji *et al.* found $E_c \approx 120$ mK (Ref. 11) and Litvin *et al.*[14] reported $E_c = 210$ mK.[14] In the single-particle interference model,[25] the decay of the interference with temperature is due to energy averaging over the temperature window $k_B T$, limiting the temporal coherence of the electron source. In a two-path interferometer with a path-length difference of ΔL, a wave with energy E will acquire a phase term in the interference signal given by $E \Delta L / \hbar v_D$ (v_D is the drift velocity), so that $E_c \approx \hbar v_D / \Delta L$. Drift velocity for edge states in the quantum-Hall regime has typical values of

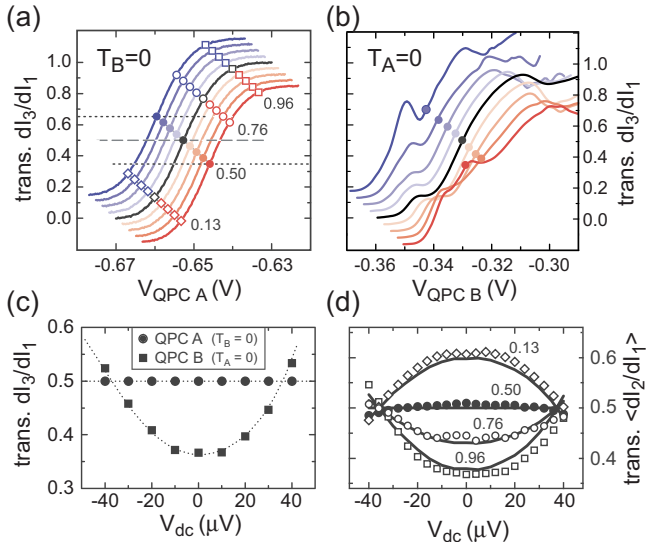

FIG. 2. (Color online) (a) Differential transmissions $T_A = dI_3/dI_1$ of the outer edge state i through the QPC A with QPC B fully reflective as a function of gate voltages $V_{\mathrm{QPC}A}$ for different dc bias voltages V_{dc} ranging between −40 to 40 μV in steps of 10 μV. The curves are offset for clarity. (b) Similar to (a) but T_B for QPC B as the variable and QPC A fully reflective. (c) Energy dependence of the differential transmission T_A of QPC A at $V_{\mathrm{QPC}A} = -0.65$ V and T_B of QPC B at $V_{\mathrm{QPC}B} = -0.33$ V. (d) The dots represent the measured total mean differential transmission $\langle dI_2/dI_1 \rangle$ through the MZI as a function of dc bias voltage V_{dc} with the gate voltage of QPC B fixed to $V_{\mathrm{QPC}B} = -0.33$ V and for four different setting of QPC A corresponding to the transmissions $T_A = 0.13$, 0.5, 0.76, and 0.96. The solid lines are calculated values using the data in (a) and (b).

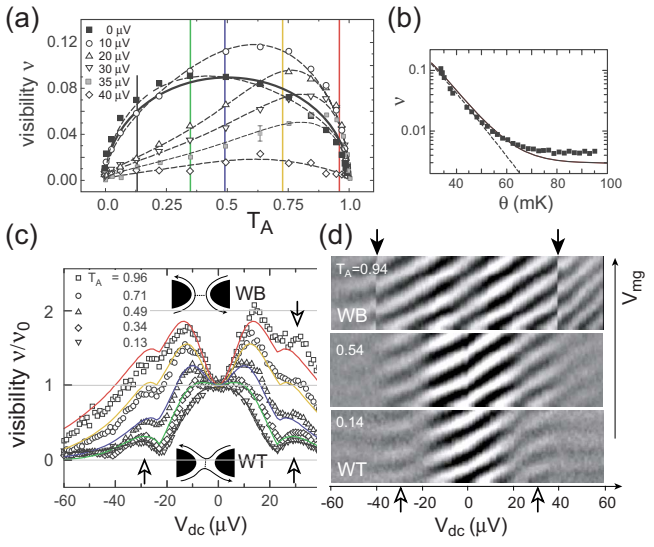

FIG. 3. (Color online) (a) Visibility ν for six different dc bias voltages as a function of the transmission probability of QPC A. The gate voltage on QPC B is fixed ($T_B = 0.56$ at $V_{dc} = 0$). (b) As a function of temperature θ, the visibility follows an exponential decay which when fitted to the dependence $\propto \exp(-k_B\theta\pi/E_c)$ yields for the characteristic energy scale E_c a value of 2.6 μeV corresponding to 30 mK. (c) The dependence of the visibility on the dc bias voltage V_{dc} scaled to the zero-bias value ν_0 for five different T_A values ($T_A = 0.96$, 0.71, 0.49, 0.34, and 0.13) and QPC B fixed as in (a). In the WB limit, the visibility first grows with increasing V_{dc}, whereas it decays in the opposite case of WT. The curves in (a) and (b) are guides for the eyes. (d) The phase evolution is visible in the measured differential transmission through the MZI as function of V_{dc} in the WB, WT, and an intermediate regime.

$10^4 - 5 \times 10^4$ m/s.[26] Using the value E_c deduced from the experiment, this then results in $\Delta L = 2.5, \ldots, 12.5$ μm. This path-length difference is unreasonably large. The MZ interferometer has been carefully designed to have the same path length on either arm. Taking the full arm length of only 15 μm, the estimated ΔL must be wrong. The reduced interference amplitude and strong temperature dependence are therefore not caused by energy self-averaging[17] but must be due to another energy-dependent decoherence mechanism. Such a mechanism may be provided by dephasing due to the electron-electron interaction.[5]

III. MEASUREMENTS AND DISCUSSION

Because we intend to vary the transmission probability of both QPCs and the dc bias voltage, the QPCs have to be carefully characterized. In order to measure the transmission characteristics of QPC A (B), the other QPC B (A) is completely closed so that all current is reflected. The current at contact 3 is then a measure of the transmission probability. In Figs. 2(a)–2(c), we present the differential transmission probability $T_{A,B} := dI_3/dI_1$ of each individual QPC at different bias voltages V_{dc} as a function of gate voltage $V_{\mathrm{QPC}A,B}$ applied to the QPCs. Whereas T_A is energy independent, T_B reveals a resonance structure at $V_{\mathrm{QPC}B} = -0.345$ V. In the experiments presented below, we varied the transmission probabilities of both QPCs over a large range. Once both point contacts are adjusted, the transmission probability of each individual QPC cannot be measured anymore. We then only have access to the mean total transmission probability $\langle T_{21} \rangle$ of the MZI between contacts 1 and 2 (or 1 and 3). In Fig. 2(d), we compare the measured mean transmission probability $\langle dI_2/dI_1 \rangle$ (symbols) with the expected value $\langle T_{21} \rangle = T_A T_B + R_A R_B$ (solid curves) using the transmission and reflection coefficients $T_{A,B}$ and $R_{A,B}$, experimentally determined before. The good agreement shows that we are able to adjust the two QPCs independently in the closed interferometer and even for $V_{dc} \neq 0$.

In Fig. 3(a), the peak-to-peak visibility ν deduced from the differential transmission probability in the outer edge state dI_2/dI_1 is shown as a function of the transmission probability of the first beam splitter at the entrance of the MZI, defined by QPC A with QPC B fixed ($T_B = 0.56$) for different dc bias voltages V_{dc}. According to the theory, ν should be proportional to $\sqrt{T_A R_A} = \sqrt{T_A(1 - T_A)}$. This dependence is shown as a solid curve. Taking the error bar of the experiment into account, a good agreement is found for the zero-bias case. In the nonequilibrium case, for bias voltages $V_{dc} \gtrsim 10$ μV a striking asymmetry appears. This asymmetry is inconsistent with the relation $\nu \propto \sqrt{T_A R_A}$, which is symmetric around 50% transmission. As compared to the equilibrium values and for not too large bias voltages, the visibility increases with V_{dc} for large T_A values, whereas it always de-

cays for small ones. This is better visible in Fig. 3(c) which shows the scaled visibility ν/ν_0 (where ν_0 is the visibility at $V_{dc}=0$) for five different settings of T_A running from top to bottom from the weak-backscattering (WB) limit in which T_A is large to the weak-tunneling (WT) limit in which T_A is small. In contrast to the WB limit, ν/ν_0 first decays with increasing $|V_{Ddc}|$ to develop a side lobe appearing symmetrically approximately at ± 30 μV on either bias side. The side lobes are visible in all curves in Fig. 3(c) (open arrows), as well as in the grayscale phase image in Fig. 3(d). Such a dependence of ν on V_{dc}, a central lobe accompanied by side lobes, has been reported in several publications.[12,14–16] In some reports, only one pair of side lobe appears, whereas in other studies several were observed. Though only one pair of side lobe is clearly visible in Fig. 3(c), the grayscale image in Fig. 3(d) suggests the appearance of a second pair at ≈ 50 μV. In addition, it has been reported that the phase of the interference pattern in a MZI can jump by π on the transition from one lobe to the other.[12,15] Bias-induced π-phase jumps where reported before in Aharanov-Bohm rings with tunneling barriers[27,28] and interpreted as the electric Aharanov-Bohm effect. Whereas the phase is seen in Fig. 3(d) to gradually evolve at small bias voltage, a more complex curved pattern is present at larger bias voltages.[28,29] However, in the WT limit, the lobe structure does not seem to be accompanied by a phase jump of π as reported by Neder *et al.*[12,15] In contrast, clear phase jumps appear in the WB limit as seen in Fig. 3(d) (filled arrow). Generally, the visibility dependence in the WB limit strongly contrasts the WT one. In the former, ν is *enhanced* for small bias voltages above the equilibrium value. At larger bias voltages, ν decays displaying a weak modulation best visible in the gray plot of Fig. 3(d). The reversed dependence on V_{dc} for small bias voltages in the two limits shows that these limits are inequivalent in the MZI with edge states. This is an effect, which one would not anticipate in a model in which the two partial beams are equivalent and isolated from the environment. Before discussing the origin of this effect, we have to prove that the effect is not induced by *one* of the QPC but is a property of the interferometer.

The discovered asymmetry in the visibility is observed in Fig. 3(a) as a function of the transmission probability T_A of QPC A, which is the first beam splitter at the entrance of the interferometer. One could argue that this effect may be a property of this particular quantum point contact. At first, this seems unlikely because QPC A is the point contact that shows a very smooth and energy-independent transition from $T_A=0$ to $T_A=1$ [Fig. 2(a)]. Second, we can revert the role of the two QPCs by changing the direction through which the current flows. This is achieved by switching the magnetic field and placing the source at contact 2. We then measure the differential transmission $T_{12}\equiv dI_1/dI_2$ from contact 2 to the drain contact 1, instead of T_{21}. Now, QPC B is the first beam splitter in the interferometer and QPC A the second one. Hence, the asymmetry in ν should show up if we now vary QPC B. This is indeed the case as demonstrated in Fig. 4(a). If, on the other hand, we vary the transmission probability of the second QPC, QPC A, a symmetric dependence of ν is found. This is shown in Fig. 4(b).

Our results clearly show that the beam splitter at the entrance determines the asymmetry and that this is independent

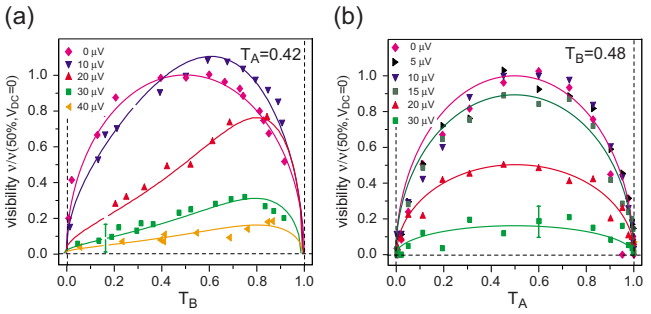

FIG. 4. (Color online) (a) Visibility ν normalized to the value observed at $T_{A,B}=0.5$ and $V_{dc}=0$ for different dc bias voltages (different labels) as a function of the transmission probability of QPC B with QPC A fixed and vice versa in (b). In these experiments, the sign of the magnetic field was reversed as well as the role of source and drain contacts. The dc bias voltage is now applied to contact 2, while contact 1 is used to measure the current. The asymmetry observed in Fig. 3(a) and the present figure (b) are determined by the first QPC but not by the second one.

on the global direction taken by the current through the interferometer. Contrary to this asymmetry, the dependence on the exit beam splitter reveals the well-known symmetric semicircle dependence. This proves that the observed asymmetric visibility dependence is a property of the interferometer and not of one of the individual QPCs.

In order to understand this effect, we have to look for a property that is different for the two partial beams. The first beam splitter divides the incident beam into two portions that propagate further along the two different paths. In the schematics of Fig. 1(a), the two paths are alike (except for the modulation gate). In the real device shown in Fig. 1(b), the two trajectories bear an additional difference which is evident if one recalls that we are working at filling factor 2. The second inner edge state *ii*, which we have ignored in the previous discussion, is differently occupied in arm a and b (see the illustration in Fig. 5) (see also Fig. 3 of Ref. 30). In arm a, it is filled up to the potential V of the source contact, i.e., it carries the full quantum current $(e^2/h)V$. In contrast, in arm b it is kept at zero potential because contact 3 is con-

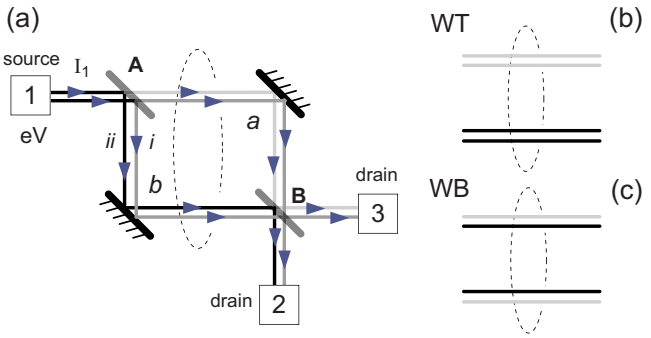

FIG. 5. (Color online) (a) Illustration of the MZI showing the two transport channels. The dark black lines indicate edge states with filling up to eV, whereas the gray one has an intermediate filling. Light gray indicates low filling. [(b) and (c)] display the fillings in the two interferometer arms in the WT and the WB regimes, respectively. See also Fig. 3 of Ref. 30.

nected to ground. In terms of state occupation, there is an asymmetry between the two arms. This asymmetry is smallest in the WB limit, where on each arm one edge state is filled up to V while the other remains "empty" (filled to zero potential). The asymmetry is largest in the opposite case of WT. In arm b, both edge states are then filled closely to zero potential whereas they are both filled to V in a. It is in this regime in which the visibility is strongly suppressed, hence, in which dephasing is large. The experiment therefore shows that the pair of edge states is most strongly susceptible to dephasing if their Fermi edges are close together. Because dephasing can efficiently be mediated by electron-electron interaction in a low-dimensional system, one could reason that the two edge states have similar group velocities at similar filling, leading to similar charge-density wave excitations. The coupling of such plasmonic charge excitation may strongly influence the coherence in the interferometer.[30,31]

That the edge state is strongly coupled electrostatically is reflected in the phase evolution. The phase in Fig. 3(d) gradually shifts with bias voltage V_{dc}. This shifts amounts to 2π for approximately 20 μV. We can understand this as an electrostatic gating from the inner edge state onto the outer one. The inner edge state ii in the outer arm a of the MZI is also biased to V_{dc} and electrostatically influences the chemical potential in the outer edge state i, which is the one taking directly part in the interference. The electrostatic phase is then given by $\alpha 2eV_{\mathrm{gate}}L/\hbar v_D$, where V_{gate} equals V_{dc}, $v_D = 10^4 - 5\times 10^4$ m/s is the drift velocity,[26] $L=15$ μm is the arm length of the interferometer, and α is the gate-coupling efficiency. With the measured values, our experiment is consistent with $\alpha = 0.14, \ldots, 0.75$ depending on the exact (but unknown) drift velocity. Because of the close proximity of the edge states, a large coupling is plausible. The strong electric coupling between the edge states may provide a channel for dephasing as proposed by Levkivskyi and Sukhorukov.[30] In their theory, the excitations are dipolar and charged edge magnetoplasmons. This theory results in a dephasing rate which is inversely proportional to the temperature θ, which was confirmed recently.[17] A similar dependence was also derived for a single channel when screening was taken into account in a self-consistent manner.[5] In the latter model, dephasing is caused by intrinsic phase fluctuations driven by the thermal bath. A related concept of intrinsic dephasing in a single channel has been put forward in two other papers recently.[32,33]

While these theories provide a mechanism for the decay of the measured visibility with θ and bias voltage V_{dc}, we also observe an increase in ν as a function of V_{dc} for certain settings of the QPCs. This can qualitatively be understood using a simple argument. We assume in the following vanishing dephasing. The detector current in the outer edge state I_2 as a function of the bias voltage V can then be written as

$$I_2(V) = \frac{e^2}{h} V[\langle T_{21}(V)\rangle + \hat{T}_{21}(V)\cos(\phi_0 + \beta V_{\mathrm{mg}} + \gamma V)], \quad (2)$$

where $\langle T_{21}(V)\rangle$ is the mean transmission, $T_{21}(V)$ is the interference amplitude, ϕ_0 is a static phase term, depending on the Aharonov-Bohm flux, and β and γ parameters that describe the coupling from the modulation gate and the inner edge state onto the phase. With the previous notation $\gamma = \alpha 2L/\hbar v_D = 0.3(\mu\mathrm{V})^{-1}$. Because we have measured the differential transmission, we have to evaluate $dI_2/dI_1 = (h/e^2)(\partial I_2/\partial V)$. It contains two interference term: $(\hat{T}_{21} + V\partial\hat{T}_{21}/\partial V)\cos(\ldots)$ and $-V\gamma\hat{T}_{21}V\gamma\sin(\ldots)$, resulting in a visibility of

$$\nu = 2\sqrt{(\hat{T}_{21} + V\,\partial\,\hat{T}_{21}/\partial V)^2 + (\hat{T}_{21}V\gamma)^2}. \quad (3)$$

Even for ideal beam splitters, for which $\hat{T}_{21}$ does not depend on V, the visibility can increase with bias voltage V due to the term $\hat{T}_{21}V\gamma$. If we assume $\partial\hat{T}_{21}/\partial V = 0$ and compare the zero-bias curvature of the $\nu/\nu_0(V_{dc})$ in Fig. 3(c) (WB curve) with Eq. (3), we deduce for γ a value of $0.15(\mu\mathrm{m})^{-1}$ which is in reasonable agreement with the value deduced from the phase shift before, i.e., $\gamma = 0.3(\mu\mathrm{V})^{-1}$. If we add in addition an exponential dephasing term with a dephasing rate proportional to V,[5,30] i.e., $\hat{T}_{21} = T_0\exp(-V/V_\phi)$, the visibility at small voltages $V \ll V_\phi$ will approximately follow $1 - V/V_\phi + (V\gamma)^2/2$ and be dominated by the exponential decay for $V \gtrsim V_\phi$. This shows that ν can indeed grow for not too large applied voltages provided that V_ϕ is large, i.e., $V_\phi > 2/V\gamma^2$. What theory has to provide is the relation between channel occupation determined by the mirror settings and the parameters γ and V_ϕ to understand the peculiar asymmetry in $\nu(T_A)$ of Fig. 3(a) and $\nu(T_B)$ of Fig. 4(a).

IV. CONCLUSION

Mach-Zehnder interferometers were proposed as building blocks for the realization of orbitally entangled states.[34,35] In order to prove the entanglement, however, one would need to analyze a Bell inequality, for which the probability for two-particle coincidences is expressed in terms of zero-frequency current-noise correlators. Such measurements are performed out of equilibrium and for many different transmission probabilities of the quantum point contacts. An understanding of the visibility at finite bias[32,33] and for different transmission probabilities is therefore crucial for future experiments along this line. On its own, the observed intrinsic asymmetry in the visibility of a MZI with edge states yields new insights in the properties edge states, in particular, in their phase coherence and mutual coupling. It would be interesting to see whether the recent theories[30,32,33] are able to reproduce the asymmetric dependence of the visibility on the mirror setting at the input of the MZI.

ACKNOWLEDGMENTS

The authors wish to thank S. Csonka, M. Büttiker, W. Dietsche, I. P. Levkivskyi, C. Strunk, E. V. Sukhorukov, P. Roche, J. Weis, and D. Zumbühl. This work was supported by the Swiss National Science Foundation and the NCCR on Nanoscale Science.

*christian.schoenenberger@unibas.ch

[1] L. Zehnder, Z. Instrumentenkd. **11**, 275 (1891).
[2] M. Born and E. Wolf, *Principles of Optics* (Cambridge University Press, Cambridge, England, 1999).
[3] A. Zeilinger, Rev. Mod. Phys. **71**, S288 (1999).
[4] A. E. Hansen, A. Kristensen, S. Pedersen, C. B. Sorensen, and P. E. Lindelof, Phys. Rev. B **64**, 045327 (2001).
[5] G. Seelig and M. Büttiker, Phys. Rev. B **64**, 245313 (2001).
[6] A. Yacoby, M. Heiblum, V. Umansky, H. Shtrikman, and D. Mahalu, Phys. Rev. Lett. **73**, 3149 (1994).
[7] A. Yacoby, M. Heiblum, D. Mahalu, and H. Shtrikman, Phys. Rev. Lett. **74**, 4047 (1995).
[8] A. Yacoby, R. Schuster, and M. Heiblum, Phys. Rev. B **53**, 9583 (1996).
[9] R. Schuster, E. Buks, M. Heiblum, D. Mahalu, V. Umansky, and H. Shtrikman, Nature (London) **385**, 417 (1997).
[10] E. Buks, R. Schuster, M. Heiblum, D. Mahalu, and H. Shtrikman, Nature (London) **391**, 871 (1998).
[11] Y. Ji, Y. Chung, D. Sprinzak, M. Heiblum, D. Mahalu, and H. Shtrikman, Nature (London) **422**, 415 (2003).
[12] I. Neder, M. Heiblum, Y. Levinson, D. Mahalu, and V. Umansky, Phys. Rev. Lett. **96**, 016804 (2006).
[13] I. Neder, M. Heiblum, D. Mahalu, and V. Umansky, Phys. Rev. Lett. **98**, 036803 (2007).
[14] L. V. Litvin, H.-P. Tranitz, W. Wegscheider, and C. Strunk, Phys. Rev. B **75**, 033315 (2007).
[15] I. Neder, F. Marquardt, M. Heiblum, D. Mahalu, and V. Umansky, Nat. Phys. **3**, 534 (2007).
[16] P. Roulleau, F. Portier, D. C. Glattli, P. Roche, A. Cavanna, G. Faini, U. Gennser, and D. Mailly, Phys. Rev. B **76**, 161309(R) (2007).
[17] P. Roulleau, F. Portier, D. C. Glattli, P. Roche, A. Cavanna, G. Faini, U. Gennser, and D. Mailly, Phys. Rev. Lett. **100**, 126802 (2008).
[18] L. V. Litvin, A. Helzel, H.-P. Tranitz, W. Wegscheider, and C. Strunk, Phys. Rev. B **78**, 075303 (2008).
[19] K. v. Klitzing, G. Dorda, and M. Pepper, Phys. Rev. Lett. **45**, 494 (1980).
[20] B. I. Halperin, Phys. Rev. B **25**, 2185 (1982).
[21] M. Büttiker, Phys. Rev. B **38**, 9375 (1988).
[22] *Springer Series in Solid-State Sciences*, edited by T. Chakraborty and P. Pietilainen (Springer, New York, 1995), Vol. 85.
[23] M. Henny, S. Oberholzer, C. Strunk, T. Heinzel, K. Ensslin, M. Holland, and C. Schönenberger, Science **284**, 296 (1999).
[24] S. Oberholzer, E. Bieri, C. Schönenberger, M. Giovannini, and J. Faist, Phys. Rev. Lett. **96**, 046804 (2006).
[25] V. S.-W. Chung, P. Samuelsson, and M. Büttiker, Phys. Rev. B **72**, 125320 (2005).
[26] S. Komiyama, H. Hirai, S. Sasa, and S. Hiyamizu, Phys. Rev. B **40**, 12566 (1989).
[27] A. van Oudenaarden, M. H. Devoret, Yu. V. Nazarov, and J. E. Mooij, Nature (London) **391**, 768 (1998).
[28] W. G. van der Wiel, Yu. V. Nazarov, S. De Franceschi, T. Fujisawa, J. M. Elzerman, E. W. G. M. Huizeling, S. Tarucha, and L. P. Kouwenhoven, Phys. Rev. B **67**, 033307 (2003).
[29] R. Leturcq, R. Bianchetti, G. Götz, T. Ihn, K. Ensslin, D. C. Driscoll, and A. C. Gossard, Physica E (Amsterdam) **35**, 327 (2006).
[30] I. P. Levkivskyi and E. V. Sukhorukov, Phys. Rev. B **78**, 045322 (2008).
[31] E. V. Sukhorukov and V. V. Cheianov, Phys. Rev. Lett. **99**, 156801 (2007).
[32] I. Neder and E. Ginossar, Phys. Rev. Lett. **100**, 196806 (2008).
[33] S.-C. Youn, H.-W. Lee, and H.-S. Sim, Phys. Rev. Lett. **100**, 196807 (2008).
[34] P. Samuelsson, E. V. Sukhorukov, and M. Büttiker, Phys. Rev. Lett. **92**, 026805 (2004).
[35] I. Neder, N. Ofek, Y. Chung, M. Heiblum, D. Mahalu, and V. Umansky, Nature (London) **448**, 333 (2007).